

**CBMS Conference: Interface of Mathematical Biology and Linear Algebra**  
**List of Projects**

Patrick De Leenheer

A Problem about the Problems with the Basic Reproduction Number

*Project Introduction: Monday May 23, 16:00-16:30 in BA1 121*

Daozhou Gao

Impact of Human Movement on Disease Persistence

*Project Introduction: check the pre-recorded video posted on conference website*

Co-leader: Guihong Fan

Stephen Kirkland

Braess' Paradox for a Random Walk on a Graph: How Bad Could It Be?

*Project Introduction: Monday May 23, 16:00-16:30 in BA1 122*

Co-leader: Xiaohong Zhang

Mark Lewis

Modelling the European Green Crab and Its Parasite Using a System of Integrodifference Equations

*\*Please check posted slides of Lectures 6 and 10 for project-related materials*

*Project Introduction: Monday May 23, 16:30-17:00 in BA1 122*

Co-leader: Yanyu Xiao

Junping Shi

Minimal Network Structure for Turing Instability

*Project Introduction: Monday May 23, 16:30-17:00 in BA1 121*

Zhisheng Shuai

Modeling Population Dynamics in Stream Environments: Impact of Movement Networks/Matrices

*Project Introduction: Monday May 23, 17:00-17:30 in BA1 122*

Co-leader: Yixiang Wu

Pauline van den Driessche

Modeling COVID-19 with Testing Regimes

*Project Introduction: Monday May 23, 17:00-17:30 in BA1 121*

Co-leader: Wenjing Zhang

# A problem about the problems with the Basic Reproduction Number

Patrick De Leenheer\*

The basic reproduction number  $R_0$  is a concept used frequently in ecology and epidemiology. Although popularized in the past few decades with the maturation of mathematical biology as an independent mathematical discipline, it is perhaps not as well-known as it should be that  $R_0$  was introduced much earlier (at least by the early 60ies) by Richard Varga [2] who was working on numerical analysis, see also [1]. Its success derives largely from the fact that it is usually easier to calculate  $R_0$  in terms of model parameters than is the spectral radius of the operator it is associated to, and, because of an important result already known to Varga [2] that says that  $R_0$  and the associated spectral radius are “on the same side of 1”. In epidemiological models for instance, this has led to the development of control strategies aimed at lowering  $R_0$ . The main idea seems to be that lowering  $R_0$  may push its value below 1 which often corresponds to stabilizing the disease-free equilibrium. But does lowering  $R_0$  always lower the associated spectral radius?

The main objective of this project is to examine this question more carefully. I will share simple examples showing that  $R_0$  could decrease whereas the spectral radius of the operator it is associated to actually increases. This suggests that one needs to be cautious when dealing with control strategies aimed at decreasing  $R_0$ , because they could potentially have the opposite effect of what they intend to achieve.

To be a bit more specific, suppose we have a linear operator  $A$  on  $\mathbb{R}^n$  which preserves a proper cone<sup>1</sup>  $C$ , i.e.  $A(C) \subset C$ . In most applications the cone  $C$  is the non-negative orthant cone  $\mathbb{R}_+^n$ , but there are examples including the Lorenz cone or the cone of positive-semidefinite symmetric matrices with more interesting geometrical properties. We shall denote the spectral radius of the operator  $A$  by  $r(A)$ . Suppose we split  $A$  as follows:

$$A = T + F,$$

where  $T$  and  $F$  also preserve the cone,  $T \neq 0$ , and  $r(T) < 1$ . It is noteworthy that this splitting of  $A$  is not unique. But corresponding to a specific splitting  $T + F$  of  $A$ , we associate a basic reproduction number  $R_0$ , defined as

$$R_0 = r(F(I - T)^{-1}),$$

i.e.  $R_0$  is the spectral radius of the operator  $F(I - T)^{-1}$ , yet another operator that preserves  $C$ . The folklore Theorem is the following Trichotomy which expresses that  $r(A)$  and  $R_0$  are “on the same side of 1”, and a bit more, namely that  $R_0$  is never closer to 1 than is  $r(A)$ .

**Theorem 1.** *Exactly one of the following 3 cases occurs:*

$$R_0 \leq r(A) < 1, \text{ or } R_0 = r(A) = 1, \text{ or } 1 < r(A) \leq R_0.$$

---

\*Department of Mathematics and Department of Integrative Biology, Oregon State University  
deleenhp@math.oregonstate.edu

<sup>1</sup>A set  $C$  in  $\mathbb{R}^n$  is a *proper cone* if it is a cone (i.e. a convex set such that  $\alpha C \subset C$  for all  $\alpha \geq 0$ ) with non-empty interior, which is also pointed (i.e.  $C \cap (-C) = \{0\}$ ).

Now assume we have a collection of linear operators  $A(t)$  on  $\mathbb{R}^n$ , where  $t$  belongs to some interval say, such that  $A(t)$  preserves a proper cone  $C$  for all  $t$ . Assume we split  $A(t)$  as follows:

$$A(t) = T(t) + F(t),$$

where  $T(t)$  and  $F(t)$  also preserve the cone  $C$ ,  $T(t) \neq 0$ , and  $r(T(t)) < 1$  for all  $t$ . As before we define  $R_0(t)$  as  $r(F(t)(I - T(t))^{-1})$ .

**The question we wish to address in this project is whether or not monotonicity of  $R_0(t)$  with respect to  $t$ , implies monotonicity of the same kind (increasing or decreasing) for  $r(A(t))$ .** As mentioned earlier the answer is no, and I will provide some simple examples to illustrate this phenomenon. On the other hand, there exist also scenarios where the answer is yes. Perhaps a more refined problem would therefore be to identify conditions on  $A(t)$ ,  $F(t)$  and  $T(t)$  for which the above implication holds.

- Students with an affinity for specific biological applications could pick their favorite ecological or epidemiological model and try to examine the above question for their model.
- Students with an affinity for linear algebra could consider cones  $C$  that are used less frequently than the non-negative orthant cone and specific collections of linear operators  $A(t)$  that preserve this cone.
- The above question is motivated by an underlying discrete model

$$x_{k+1} = Ax_k,$$

where  $k$  is a non-negative integer,  $x_k$  belongs to  $C$ , and  $A$  preserves  $C$ . In epidemiology in particular, one typically considers differential equation models instead. These are obtained by linearization at the disease-free steady states of the epidemiological models and they take the form

$$\dot{x} = Ax,$$

where  $x$  belongs to  $C$ , and  $A$  is the generator of a semigroup  $e^{tA}$  which preserves the cone  $C$  for all  $t \geq 0$ . A different splitting of  $A$  then leads to a somewhat different-looking definition of  $R_0$ : One writes  $A = F - V$  where  $F$  and  $V$  satisfy certain conditions, and defines  $R_0$  as  $r(FV^{-1})$ . Students could “translate” the above question and examine it in this context of differential equation models.

## References

- [1] J.S. Vandergraft, Spectral properties of matrices which have invariant cones, SIAM Journal of Applied Mathematics 16, p. 1208-1222, 1968.
- [2] R. S. Varga, Matrix Iterative Analysis, Prentice-Hall, Englewood Cliffs, New Jersey, 1963.

# Impact of Human Movement on Disease Persistence

Daozhou Gao<sup>1</sup>

<sup>1</sup>Department of Mathematics, Shanghai Normal University, Shanghai 200234, China

Infectious diseases can be easily spread from one region to another through population dispersal. Due to globalization, urbanization and transportation development, more people traveled more frequently and farther over the past few decades. Travel restrictions, lockdowns and stay at home orders during the COVID-19 pandemic significantly reduce human mobility. It is important to understand how changes in travel behavior affect the disease persistence which can be measured by the basic reproduction number  $\mathcal{R}_0$ . Usually, a disease dies out if  $\mathcal{R}_0 < 1$  and spreads out otherwise. Thus, it is feasible to determine the outcome of disease spread through analyzing the dependence of  $\mathcal{R}_0$  on travel-related parameters.

## 1 SIS Patch Model

We consider a discrete space consisting of  $n \geq 2$  patches. Let  $S_i$  and  $I_i$  be the number of susceptible and infectious individuals in patch  $i \in \Omega = \{1, \dots, n\}$ . In 2007, Allen et al. [1] proposed an SIS patch model

$$\begin{aligned} \frac{dS_i}{dt} &= -\beta_i \frac{I_i}{S_i + I_i} S_i + \gamma_i I_i + \delta \sum_{j \in \Omega} L_{ij} S_j, \quad i \in \Omega, \\ \frac{dI_i}{dt} &= \beta_i \frac{I_i}{S_i + I_i} S_i - \gamma_i I_i + \varepsilon \sum_{j \in \Omega} L_{ij} I_j, \quad i \in \Omega, \end{aligned} \tag{1.1}$$

where  $\delta$  and  $\varepsilon$  are the dispersal rates of the susceptible and infectious populations, respectively. In patch  $i$ , the parameters  $\beta_i$  and  $\gamma_i$  are the transmission coefficient and recovery rate, respectively;  $L_{ij}$  is the degree of incoming movement from patch  $j$  to patch  $i$  and  $L_{ji}$  is the degree of outgoing movement from patch  $i$  to patch  $j$  for  $i \neq j$ . It is assumed that the connectivity matrix  $L = (L_{ij})_{n \times n}$  is essentially nonnegative and irreducible with zero column sums.

The basic reproduction number of model (1.1) is

$$\mathcal{R}_0 = \rho(FV^{-1}),$$

where

$$F = \text{diag}(\beta_1, \dots, \beta_n) \quad \text{and} \quad V = \text{diag}(\gamma_1, \dots, \gamma_n) - \varepsilon L.$$

Allen et al. [1] conjectured that  $\mathcal{R}_0$  is a monotone decreasing function of  $\varepsilon$ . This was recently proved by Gao [3], Gao and Dong [4], and Chen et al. [2]. Namely, if  $\mathcal{R}_0^{(i)}$  is constant in  $i \in \Omega$ , then  $\mathcal{R}_0$  is constant in  $\varepsilon$ ; otherwise,  $\mathcal{R}_0$  is strictly decreasing in  $\varepsilon$ . Biologically speaking, fast dispersal reduces disease persistence.

In reality, there are different levels of unilateral, bilateral, and multilateral connection among different countries or regions. It is necessary to consider how disease persistence varies with partial changes in connection, e.g.,  $\mathcal{R}_0$  versus  $s$  where  $L_{ij} = sK_{ij}$  for

- (i) a fixed pair of  $i$  and  $j$  with  $i \neq j$ ;
- (ii) a given  $i$  and all  $j \neq i$ , or a given  $j$  and all  $i \neq j$ ;
- (iii) all  $i, j \in \Omega_1 \subset \Omega$  and  $i \neq j$ .

So far very limited studies have been carried out (see Gao and Ruan [6, 7]). Moreover, the role of network topology and connectivity on disease spread also deserves investigation [9].

## 2 SEIRS Patch Model

Recently, based on an SEIRS reaction-diffusion model, Song et al. [10] studied the monotonicity of the reproduction number with respect to the diffusion rates of the exposed and infectious individuals. We consider the associated but generalized SEIRS patch model

$$\begin{aligned}
\frac{dS_i}{dt} &= d_S \sum_{j \in \Omega} L_{ij}^S S_j - \beta_i \frac{S_i I_i}{S_i + E_i + I_i + R_i} + \alpha_i R_i, \quad i \in \Omega, \\
\frac{dE_i}{dt} &= d_E \sum_{j \in \Omega} L_{ij}^E E_j + \beta_i \frac{S_i I_i}{S_i + E_i + I_i + R_i} - \sigma_i E_i, \quad i \in \Omega, \\
\frac{dI_i}{dt} &= d_I \sum_{j \in \Omega} L_{ij}^I I_j + \sigma_i E_i - \gamma_i I_i, \quad i \in \Omega, \\
\frac{dR_i}{dt} &= d_R \sum_{j \in \Omega} L_{ij}^R R_j + \gamma_i I_i - \alpha_i R_i \quad i \in \Omega,
\end{aligned} \tag{2.1}$$

where  $\sigma_i$  is the rate that exposed individuals become infectious and  $\alpha_i$  is the rate of loss of immunity. The dispersal rate and connectivity matrix of the susceptible, exposed, infectious and recovered people are  $d_{\mathfrak{h}}$  and  $L^{\mathfrak{h}} = (L_{ij}^{\mathfrak{h}})$  with  $\mathfrak{h}$  denoting  $S, E, I$  and  $R$ , respectively. For simplicity,  $L^{\mathfrak{h}}$  is assumed to be essentially nonnegative and irreducible with zero column sums for  $\mathfrak{h} \in \{S, E, I, R\}$ .

The incidence and transition matrices are respectively

$$F = \begin{pmatrix} 0 & F_{12} \\ 0 & 0 \end{pmatrix} \text{ and } V = \begin{pmatrix} V_{11} & 0 \\ V_{21} & V_{22} \end{pmatrix},$$

where  $F_{12} = \text{diag}\{\beta_1, \dots, \beta_n\}$ ,  $V_{11} = \text{diag}\{\sigma_1, \dots, \sigma_n\} - d_E L^E$ ,  $V_{21} = -\text{diag}\{\sigma_1, \dots, \sigma_n\}$  and  $V_{22} = \text{diag}\{\gamma_1, \dots, \gamma_n\} - d_I L^I$ . Using the next generation matrix method, the basic reproduction number of model (2.1) is defined as

$$\mathcal{R}_0 = \rho(FV^{-1}) = \rho(-F_{12}V_{22}^{-1}V_{21}V_{11}^{-1}).$$

By a simple comparison principle, we can show that the disease-free equilibrium is globally asymptotically stable if  $\mathcal{R}_0 \leq 1$ ; by the persistent theory, the disease is uniformly persistent and there exists at least one endemic equilibrium if  $\mathcal{R}_0 > 1$ . So, the disease dynamics are completely governed by the reproduction number and we wonder how population migration impacts  $\mathcal{R}_0$ . Some research questions:

- (i) The basic reproduction number of model (2.1) satisfies

$$\min_{1 \leq i \leq n} \mathcal{R}_0^{(i)} \leq \mathcal{R}_0 \leq \max_{1 \leq i \leq n} \mathcal{R}_0^{(i)},$$

where  $\mathcal{R}_0^{(i)} = \beta_i/\gamma_i$  is the reproduction number of patch  $i$  in isolation.

- (ii) Give some sufficient conditions under which  $\mathcal{R}_0$  is strictly decreasing in  $d_E$  and/or  $d_I$ .
- (iii) Completely determine the monotonicity of  $\mathcal{R}_0$  in  $d_E$  and  $d_I$  for the two-patch case.
- (iv) Find the necessary and sufficient conditions under which  $\mathcal{R}_0$  is independent of dispersal rates or dispersal.
- (iv) Analytically and numerically explore the effects of population movement on disease prevalence (including the asymptotic profiles of the endemic equilibrium).

We plan to establish some deeper and better results than these obtained by Song et al. [10]. Some idea and approach from our recent work on an SIAR patch model [5] can be adopted.

### 3 Connectivity Matrix

Given any strictly positive vector  $\mathbf{x} = (x_1, \dots, x_n)^T$ , find all connectivity matrices  $M$  (essentially nonnegative, irreducible with zero column sums) or bases having  $\mathbf{x}$  as their right eigenvector corresponding to zero eigenvalue, i.e.,  $M\mathbf{x} = \mathbf{0}$ . For example,

$$-\sum_{i=1}^n x_i I_n + \begin{pmatrix} x_1 & x_1 & \cdots & x_1 \\ x_2 & x_2 & \cdots & x_2 \\ \vdots & \vdots & \ddots & \vdots \\ x_n & x_n & \cdots & x_n \end{pmatrix}$$

and

$$\begin{pmatrix} -x_1^{-1} & x_2^{-1} & 0 & \cdots & 0 \\ 0 & -x_2^{-1} & x_3^{-1} & \cdots & 0 \\ \vdots & \vdots & \vdots & \ddots & \vdots \\ x_1^{-1} & 0 & 0 & \cdots & -x_n^{-1} \end{pmatrix}.$$

Obviously, the positive linear combination of connectivity matrices is still a connectivity matrix. So, it suffices to find the ‘‘bases’’. The answer is applicable to the multipatch Ross–Macdonald model where the reproduction number attains its minimum as the distributions of hosts and vectors are proportional (see Remark 2 in Gao et al. [8]).

## References

- [1] L. J. S. Allen, B. M. Bolker, Y. Lou, and A. L. Nevai. Asymptotic profiles of the steady states for an SIS epidemic patch model. *SIAM J. Appl. Math.*, 67(5):1283–1309, 2007.
- [2] S. Chen, J. Shi, Z. Shuai, and Y. Wu. Asymptotic profiles of the steady states for an SIS epidemic patch model with asymmetric connectivity matrix. *J. Math. Biol.*, 80(7):2327–2361, 2020.
- [3] D. Gao. Travel frequency and infectious diseases. *SIAM J. Appl. Math.*, 79(4):1581–1606, 2019.
- [4] D. Gao and C.-P. Dong. Fast diffusion inhibits disease outbreaks. *Proc. Amer. Math. Soc.*, 148(4):1709–1722, 2020.
- [5] D. Gao, J. Munganga, P. van den Driessche, and L. Zhang. Effects of asymptomatic infections on the spatial spread of infectious diseases. *SIAM J. Appl. Math.*, in press.
- [6] D. Gao and S. Ruan. An SIS patch model with variable transmission coefficients. *Math. Biosci.*, 232(2):110–115, 2011.
- [7] D. Gao and S. Ruan. A multipatch malaria model with logistic growth populations. *SIAM J. Appl. Math.*, 72(3):819–841, 2012.
- [8] D. Gao, P. van den Driessche, and C. Cosner. Habitat fragmentation promotes malaria persistence. *J. Math. Biol.*, 79(6–7):2255–2280, 2019.
- [9] H. Jiang, K.-Y. Lam, and Y. Lou. Three-patch models for the evolution of dispersal in advective environments: Varying drift and network topology. *Bull. Math. Biol.*, 83:109, 2021.
- [10] P. Song, Y. Lou, and Y. Xiao. A spatial SEIRS reaction-diffusion model in heterogeneous environment. *J. Differential Equations*, 267(9):5084–5114, 2019.

# Braess' paradox for a random walk on a graph: how bad could it be?

Steve Kirkland

Department of Mathematics, University of Manitoba, Winnipeg, MB, Canada

## 1 Introduction

Connections are important, but they can affect network structure in unexpected ways. For example, Braess' paradox [1] is the name given to the unexpected situation in which the addition of a new route into a vehicle traffic network has the effect of *increasing* travel times. This project explores an analogue of Braess' paradox in the context of Markov chains. (Side note: Markov chains will be discussed extensively in Lecture 5.)

Specifically, we consider a connected undirected graph  $G$  on vertices labelled  $1, \dots, n$ . Associated with  $G$  is a random walk; this is a special type of Markov chain in which the random walker begins at an initial vertex  $j_0$  of  $G$ , and proceeds as follows: if the random walker is at vertex  $j_k$  at time  $k$ , it selects one of the neighbours of  $j_k$  at random, and moves to that vertex at time  $k + 1$ . (One may think of an intruder entering a network and randomly wandering from one vertex to another.)

The key properties of the random walk are captured by the corresponding transition matrix,  $T$ , which can be written as  $D^{-1}A$ , where:

- i)  $A$  is the adjacency matrix for  $G$ , i.e.  $a_{jk} = 1$  if vertices  $j$  and  $k$  are adjacent and  $a_{jk} = 0$  otherwise;
- ii)  $D$  is the diagonal matrix of vertex degrees, i.e.  $D = \text{diag}(A\mathbf{1})$ , where  $\mathbf{1}$  denotes the all-ones vector.

Evidently  $T$  is a nonnegative matrix, and each of its row sums is equal to 1. Observe that 1 is an eigenvalue of  $T$ , since  $T\mathbf{1} = \mathbf{1}$ . In the language of Lecture 1, the Perron value of  $T$  is 1 and  $\mathbf{1}$  is a corresponding right Perron vector.



The long-term properties of the random walk are reflected in the stationary distribution for  $T$ : this is the left eigenvector  $w^T$  of  $T$  corresponding to the eigenvalue 1, normalized so that its entries sum to 1. (In particular,  $w^T$  is a left Perron vector for  $T$ .) It is not hard to show that  $w^T = \frac{1}{\mathbf{1}^T D \mathbf{1}} \mathbf{1}^T D$ , so that in fact the stationary distribution  $w^T$  is governed by the vertex degrees in  $G$ . Since the entries of  $w^T$  are positive and sum to 1, we can interpret the stationary distribution as a probability distribution on  $\{1, \dots, n\}$ .

The short-term properties of the random walk are captured by its mean first passage times. The mean first passage time from vertex  $j$  to vertex  $k$ ,  $m_{jk}$ , is the expected number of steps required for the random walker to reach vertex  $k$  for the first time, given that the walker started at vertex  $j$ . Informally we may think of these first passage times as ‘travel times’ for the random walker. The entries in the stationary distribution and the mean first passage times are the ingredients used in defining Kemeny’s constant  $\kappa(G)$  for the graph  $G$  ([2]):

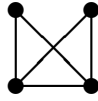
$$\kappa(G) + 1 = \sum_{j,k=1,\dots,n} w_j m_{jk} w_k.$$

Inspecting the formula for Kemeny’s constant, we see that  $\kappa(G)$  measures the expected number of steps required by a random walker to move from a randomly chosen initial vertex (i.e. randomly chosen according to the stationary distribution) to a randomly chosen final vertex (again, chosen according to the stationary distribution). Evidently Kemeny’s constant can be regarded as a measure of overall transit time for the random walk on  $G$ .

What happens when a new edge is added into a graph? Generically we expect that this overall transit time will decrease, as the new edge offers our random walker more routes with which to move around the graph. That intuition is supported by the fact that over all graphs on  $n$  vertices, Kemeny’s constant is minimized by the complete graph on  $n$  vertices (in other words, the graph with all possible edges).

Let’s look at a couple of examples.

### Example A



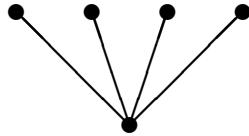
$$\text{Kemeny's constant} = \frac{47}{20}$$



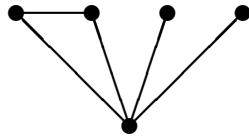
$$\text{Kemeny's constant} = \frac{9}{4}$$

In Example A we see that the behaviour conforms with our intuition – adding the new edge decreases the value of Kemeny’s constant.

### Example B



$$\text{Kemeny's constant} = \frac{7}{2}$$



$$\text{Kemeny's constant} = \frac{11}{3}$$

Example B illustrates an analogue of Braess’ paradox for graphs. That is, the addition of the new edge has the counterintuitive effect of increasing Kemeny’s constant; such an edge is known as a Braess edge. There are several known examples of families of graphs having Braess edges. For example in [5] it is shown that fraction of trees on  $n$  vertices having a Braess edge tends to 1 as  $n \rightarrow \infty$ .

**Example C** Consider the  $K_{9,9}$ , the complete bipartite graph on 18 vertices. Here the vertices are partitioned into two sets  $S_1 = \{1, \dots, 9\}$ ,  $S_2 = \{10, \dots, 18\}$ , and there's an edge between vertices  $j$  and  $k$  if and only if one of  $j, k$  is in  $S_1$  and the other is in  $S_2$ . It turns out that  $\kappa(K_{9,9}) = \frac{33}{2}$ .

Now pick two distinct indices  $j_1, j_2 \in S_1$ , and let  $G$  be the graph formed from  $K_{9,9}$  by adding the edge between  $j_1$  and  $j_2$ . Then  $\kappa(G) = \frac{14900}{903} > \kappa(K_{9,9})$ .

Example C shows that it's possible for a single graph to have many Braess edges.

## 2 Questions

1. Suppose that our graph  $G$  has a Braess edge,  $e$ , so that  $\kappa(G \cup \{e\}) > \kappa(G)$ . How large can the increase in Kemeny's constant be? A general line of inquiry is to look for an upper bound on  $\kappa(G \cup \{e\}) - \kappa(G)$ . There is a combinatorial formula for  $\kappa(G)$  (see [5]) and analysing it may yield some insights that would lead to an upper bound.

2. For some nicely structured families of graphs, for example trees, Question 1 may be tractable and would furnish insight into the general case.

3. An analytic approach may also be productive. One can think of adding the new edge with a positive weight  $x$ , then find an upper bound on the derivative of Kemeny's constant with respect to  $x$ . The group inverse of  $I - T$  is expected to be an important tool in this approach. (The group inverse is covered in Lecture 9.)

4. There is an analogue of this entire development for directed graphs, and Questions 1–3 can also be explored in the directed case.

## References

- [1] D. Braess, A. Nagurney and T. Wakolbinger, On a paradox of traffic planning, *Transportation Science* 39 (2005), 446–450.
- [2] M. Levene and G. Loizou, Kemeny's Constant and the Random Surfer, *American Mathematical Monthly* 109 (2002), 741–745.
- [3] J. Kemeny and J. Snell, *Finite Markov Chains*, Springer–Verlag, New York, 1976.

- [4] S. Kirkland and M. Neumann, *Group Inverses of M-matrices and Their Applications*, CRC Press, Boca Raton, 2013.
- [5] S. Kirkland and Z. Zeng, Kemeny's constant and an analogue of Braess' paradox for trees, *Electronic Journal of Linear Algebra* 31 (2016), 444–464.

## Group Project for CBMS Conference Interface of Mathematical Biology and Linear Algebra

Title: Modelling the European green crab and its parasite using a system of integrodifference equations.

Author: Mark Lewis

Description: European green crab (*Carcinus maenas*) is an aquatic invader. It feeds on native animals, destroys shellfish beds and outcompetes native crab species for food. It has invaded sites on both the east and west coast of North America, spreading spatially along coastal ecosystems, which often have directional currents.

A number of authors have modelled the spread of green crab using integrodifference equations. A useful reference to start with is Marculis and Lui (2016), but there are many others also. The green crab has juvenile and adult stages, connected via larval dispersal, which occurs after yearly reproduction events. Although they live in many habitats, they prefer eelgrass (*Zostera marina*) beds. To start

- Write down an integrodifference model for the green crab juvenile and adult stages. Construct a dispersal kernel as we did in Lecture 10. Consider two possibilities (i) an “infinitely” long patch of coastal habitat (ii) an isolated patch of eelgrass outside of which the habitat is hostile. What are the appropriate “boundary conditions” associated with the edge of the eelgrass habitat? Consider different possibilities. Also, be sure to include a saturating growth function for the dynamics.
- Calculate the trivial and nontrivial spatially homogeneous equilibria for this model. Are they stable?
- Calculate the up- and down-stream spreading speeds on the infinite domain for green crab, into and away from the directional current flow, following the ideas of Lectures 6 and 10. You may want to read details of similar calculations in Huang *et al.* (2017).
- Calculate the critical patch size/critical water current speed for green crab on a patch of eel grass. You have the option of whether you would like to formulate this as a classical critical patch size problem or a spatial  $R_0$  problem. What size does the patch need to be and/or what is the critical current speed? Is it possible to connect this calculation to the spreading speed(s) calculation above?
- It is possible to connect the eigenvalue for the critical patch size problem to a modification of eigenvalue for the nonspatial problem via a so-called *dispersal success approximation*. This is described nicely in the recent textbook by Frithjof Lutscher (2019). Try this approximation and see how good a job it does at estimating the critical patch size.

If you have time, consider the biological control agent, *Sacculina carcini*. This parasitic castrator of green crabs prevents the crab from moulting and reproducing. This agent has been modelled mathematically. (Again, see for example, Marculis and Lui, 2016.) Now consider the case where the green crab has already invaded a patch of eel grass. To simplify assume that the green crab has reached a spatially homogeneous equilibrium within the patch. Can the castrator invade and establish itself in the patch, potentially driving down the green crab population and helping preserve the eelgrass bed? Could there possibly be patches of certain sizes that will support the crab but not the control agent? What are the implications?

Note, only enough references have been given to get started, but you should be able to find many more in the literature.

References:

Lutscher F. Integrodifference equations in spatial ecology. Springer International Publishing; 2019.

Huang Q, Wang H, Lewis MA. A hybrid continuous/discrete-time model for invasion dynamics of zebra mussels in rivers. SIAM Journal on Applied Mathematics. 2017;77(3):854-80.

Marculis NG, Lui R. Modelling the biological invasion of *Carcinus maenas* (the European green crab). Journal of Biological Dynamics. 2016 Jan 1;10(1):140-63.

# Minimal network structure for Turing instability\*

Junping Shi<sup>1</sup>

<sup>1</sup> Department of Mathematics, William & Mary, Williamsburg, Virginia, 23187-8795, USA

Reaction-diffusion partial differential equation models have been used to describe the formation of spatiotemporal patterns in biology, chemistry and physics. Alan Turing [15] proposed that different diffusion coefficients of a pair of chemicals in a biochemical system are responsible for the generation of spatially inhomogeneous patterns, and this diffusion-induced instability (Turing instability) has been credited as one of the most important driving mechanisms of pattern formations [7].

The Turing instability is caused by the destabilization of a constant equilibrium solution  $U = U_0$  of a spatially homogeneous reaction-diffusion system  $U_t = P\Delta U + g(U)$  with  $n$  ( $\geq 2$ ) variables and coupled with proper boundary conditions, where  $U = U(x, t)$  with  $t > 0$ ,  $x$  belongs to a spatial domain,  $P$  is a diagonal  $n \times n$  matrix with non-negative diagonal entries (diffusion coefficients), and  $g$  is a smooth nonlinear vector function satisfying  $g(U_0) = 0$ . Through the techniques of linearization, the stability of the equilibrium  $U = U_0$  is reduced to a linear system of diffusion equations  $V_t = P\Delta V + AV$ , where  $A = g'(U_0)$  is a real-valued  $n \times n$  Jacobian matrix. The constant equilibrium  $U_0$  is asymptotically stable if each solution  $V$  of the linearized diffusion system converges to zero uniformly as  $t \rightarrow \infty$ . From the theory of linear differential equations, this is equivalent to the condition that each eigenvalue of the matrix  $A - \mu_j P$  has negative real part, where  $\mu_j$  ( $j = 0, 1, 2, \dots$ ) are the eigenvalues of the Laplace operator with compatible boundary conditions, and  $\mu_j$  satisfy  $0 = \mu_0 < \mu_1 \leq \mu_2 \leq \dots$  and  $\lim_{j \rightarrow \infty} \mu_j = \infty$  [12, 15].

Because of the wide applicability of Turing instability, there has been considerable interest in the study of stable matrices and stable matrices exhibiting Turing instability [9, 14]. Many realistic biological reaction mechanisms involve a large number of chemical reactants and a complex biological regulatory network. It is important to identify the key components of the biological network that is capable of generating desired patterns, and it is also important to classify minimal biological network for pattern formation [16].

To capture the behavior of the model relating to or describing the network connection of the different components, we need the following definitions. Let  $M_n$  be the set of all  $n \times n$  matrices with real-valued entries. A matrix  $A \in M_n$  is said to be *stable* if for each of its eigenvalues  $\lambda_j$  ( $j = 0, 1, 2, \dots, n$ ),  $\text{Re}(\lambda_i) < 0$ . We define the *sign pattern* of a matrix  $A = [a_{jk}]$  to be an  $n \times n$  matrix  $S(A) = [s_{jk}]$  such that, for  $j, k \in \{1, \dots, n\}$ ,  $s_{jk} = 0$  when  $a_{jk} = 0$ ,  $s_{jk} = -$  when  $a_{jk} < 0$ , and  $s_{jk} = +$  when  $a_{jk} > 0$ . We also define the *non-zero pattern* of  $A$  to be an  $n \times n$  matrix

---

\*partially based on [6]

$N(A) = [n_{jk}]$  such that, for  $j, k \in \{1, \dots, n\}$ ,  $n_{jk} = 0$  when  $a_{jk} = 0$ , and  $n_{jk} = *$  when  $a_{jk} \neq 0$ . A non-zero pattern of  $A$  can be assigned  $\pm$  signs so it becomes a sign pattern. If some matrix  $A \in M_n$  is found to be stable, then the sign pattern  $S(A)$  is said to be *potentially stable*. For a stable  $n \times n$  matrix  $A$ , if there is a nonnegative  $n \times n$  diagonal matrix  $P$  such that the matrix  $A - tP$  is unstable for some positive  $t > 0$ , then  $A$  is said to exhibit *Turing Instability*. We are interested in the minimum number of nonzero entries of a stable matrix in  $M_n$ , which will exhibit Turing instability. We will consider the minimal number  $S_n$  of nonzero entries that an  $n \times n$  irreducible matrix  $A$  must have in order for it to exhibit Turing instability.

An  $n \times n$  sign pattern  $S(A)$  with only  $S_n$  nonzero entries can be considered as a minimal network topology generating Turing instability. Turing's original work on the subject [15] implies that  $S_2 = 4$ . Indeed it is well-known that up to a permutation or transpose, the only  $2 \times 2$  sign pattern that can possibly generate Turing instability is the activator-inhibitor type  $\begin{bmatrix} - & + \\ - & + \end{bmatrix}$ . A related index is the minimum number of nonzero entries required for an  $n \times n$  irreducible sign pattern to be potentially stable, and it is denoted by  $m_n$ . Note that, trivially,  $m_n \leq S_n$  for any  $n$  since  $A$  is assumed to be stable. The known results about  $S_n$  and  $M_n$  are summarized in the following table:

$n$	2	3	4	5	6	7	8	upper bound
$M_n$	3	5	6	8	9	11	12	$\leq 2n - 1 - \lfloor \frac{n}{3} \rfloor$
$S_n$	4	6	7	8?	10?			$\leq 2n + 1 - \lfloor \frac{n}{3} \rfloor$

The results for  $M_n$  were proved in [4] for  $n \leq 6$  and the general upper bound, [5] for  $n = 7$  and [1] for  $n = 8$ . The results for  $S_3$  and general upper bound of  $S_n$  were proved in [6], and the conjecture of  $S_n$  for  $n \geq 4$  was given by Diego [2]. The result that  $S_4 = 7$  was recently verified in [10].

In the 2014 paper by Raspopovic et.al. [13], it was claimed that in order for an irreducible  $3 \times 3$  matrix to exhibit Turing instability, it must have at least 6 nonzero entries. But the claim was not proved in the paper. The result in [6] provided theoretical justification for that claim, and all distinct irreducible  $3 \times 3$  non-zero patterns with 6 non-zero entries (up to a permutation or transpose) were also classified (see Table 1). Note that the seven non-zero patterns in Table 1 were found in [3] Fig. 5. In [13], the diagonal matrix  $P$  is assumed to be  $\text{diag}(p_1, p_2, 0)$  while our results hold for any nonnegative (including positive) diagonal matrix  $P$ . The graph-theoretical methods to analyze network topologies for Turing instability were also used in [3, 8, 11].

Each of the seven non-zero patterns listed in Table 1 can be realized by one or more sign patterns and matrices exhibiting Turing instability. All non-equivalent sign patterns are listed in the following Table 2.

### Questions.

1. Rigorously determine  $S_5$ , and classify all distinct irreducible  $5 \times 5$  non-zero patterns with  $S_5$  non-zero entries. It is conjectured that  $S_5 = 8$  [2], which will provide first example that  $S_n = M_n$ . For  $2 \leq n \leq 4$ , it is known that  $S_n > M_n$ .



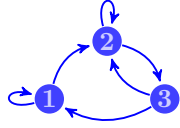
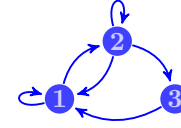
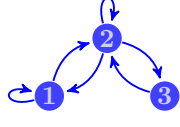
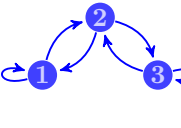
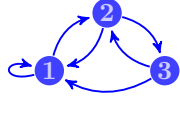
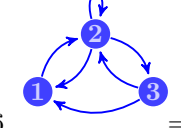
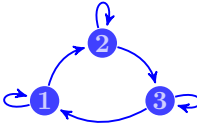
1. 	$\Rightarrow$ $\begin{bmatrix} * & * & 0 \\ 0 & * & * \\ * & * & 0 \end{bmatrix}$	2. 	$\Rightarrow$ $\begin{bmatrix} * & * & 0 \\ * & * & * \\ * & 0 & 0 \end{bmatrix}$
3. 	$\Rightarrow$ $\begin{bmatrix} * & * & 0 \\ * & * & * \\ 0 & * & 0 \end{bmatrix}$	4. 	$\Rightarrow$ $\begin{bmatrix} * & * & 0 \\ * & 0 & * \\ 0 & * & * \end{bmatrix}$
5. 	$\Rightarrow$ $\begin{bmatrix} * & * & 0 \\ * & 0 & * \\ * & * & 0 \end{bmatrix}$	6. 	$\Rightarrow$ $\begin{bmatrix} 0 & * & 0 \\ * & * & * \\ * & * & 0 \end{bmatrix}$
7. 	$\Rightarrow$ $\begin{bmatrix} * & * & 0 \\ 0 & * & * \\ * & 0 & * \end{bmatrix}$		

Table 1: List of potential digraphs with 3 vertices and 6 edges.

$\begin{bmatrix} - & + & 0 \\ 0 & - & + \\ - & + & 0 \end{bmatrix}$	$\begin{bmatrix} - & + & 0 \\ 0 & + & + \\ + & - & 0 \end{bmatrix}$	$\begin{bmatrix} + & + & 0 \\ 0 & - & + \\ - & - & 0 \end{bmatrix}$	$\begin{bmatrix} - & + & 0 \\ - & + & + \\ - & 0 & 0 \end{bmatrix}$	$\begin{bmatrix} - & + & 0 \\ + & - & + \\ 0 & - & 0 \end{bmatrix}$
(a)	(b)	(c)	(d)	(e)
$\begin{bmatrix} - & + & 0 \\ - & + & + \\ 0 & - & 0 \end{bmatrix}$	$\begin{bmatrix} + & + & 0 \\ - & - & + \\ 0 & + & 0 \end{bmatrix}$	$\begin{bmatrix} - & + & 0 \\ - & 0 & + \\ 0 & + & - \end{bmatrix}$	$\begin{bmatrix} + & + & 0 \\ - & 0 & + \\ 0 & - & - \end{bmatrix}$	$\begin{bmatrix} - & + & 0 \\ + & 0 & + \\ + & - & 0 \end{bmatrix}$
(f)	(g)	(h)	(i)	(j)
$\begin{bmatrix} - & + & 0 \\ - & 0 & + \\ - & + & 0 \end{bmatrix}$	$\begin{bmatrix} 0 & + & 0 \\ - & - & + \\ - & + & 0 \end{bmatrix}$	$\begin{bmatrix} - & + & 0 \\ 0 & + & + \\ - & 0 & - \end{bmatrix}$		
(k)	(l)	(m)		

Table 2: Nonequivalent sign patterns that are potentially exhibiting Turing Instability.

- It is observed [2] that for  $n = 2$  and  $n = 3$ , a minimal network structure for Turing instability satisfies  $S_n = n + C_n - 1$ , where  $C_n$  is the number of cycles in the minimal network with  $n$  vertices. Prove (or disprove) this relation  $S_n = n + C_n - 1$  for  $n \geq 5$ .
- Find the exact values of  $M_n$  for  $n \geq 9$  and  $S_n$  for  $n \geq 5$ .

## References

- [1] M. Cavers. Polynomial stability and potentially stable patterns. *Linear Algebra Appl.*, 613:87–114, 2021.
- [2] X. Diego. private communication. September 2021.
- [3] X. Diego, L. Marcon, P. Müller, and J. Sharpe. Key features of Turing systems are determined purely by network topology. *Physical Review X*, 8(2):021071, 2018.
- [4] D. A. Grundy, D. D. Olesky, and P. van den Driessche. Constructions for potentially stable sign patterns. *Linear Algebra Appl.*, 436(12):4473–4488, 2012.
- [5] C. L. Hambric, C.-K. Li, D. C. Pelejo, and J. Shi. Minimum number of non-zero-entries in a  $7 \times 7$  stable matrix. *Linear Algebra Appl.*, 572:135–152, 2019.
- [6] C. L. Hambric, C.-K. Li, D. C. Pelejo, and J. Shi. Minimum number of non-zero-entries in a stable matrix exhibiting Turing instability. *Discrete Contin. Dyn. Syst. Ser. S*, 2022 (to appear).
- [7] P. Maini, K. Painter, and H. P. Chau. Spatial pattern formation in chemical and biological systems. *Journal of the Chemical Society, Faraday Transactions*, 93(20):3601–3610, 1997.
- [8] L. Marcon, X. Diego, J. Sharpe, and P. Müller. High-throughput mathematical analysis identifies Turing networks for patterning with equally diffusing signals. *Elife*, 5:e14022, 2016.
- [9] J. Maybee and J. Quirk. Qualitative problems in matrix theory. *SIAM Rev.*, 11:30–51, 1969.
- [10] B. Millis and J. Shi. Minimum number of non-zero-entries in a stable  $4 \times 4$  matrix exhibiting Turing instability. 2022.
- [11] M. Mincheva and M. R. Roussel. A graph-theoretic method for detecting potential Turing bifurcations. *The Journal of Chemical Physics*, 125(20):204102, 2006.
- [12] J. D. Murray. *Mathematical Biology. II. Spatial models and biomedical applications*, volume 18 of *Interdisciplinary Applied Mathematics*. Springer-Verlag, New York, third edition, 2003.
- [13] J. Raspopovic, L. Marcon, L. Russo, and J. Sharpe. Digit patterning is controlled by a Bmp-Sox9-Wnt Turing network modulated by morphogen gradients. *Science*, 345(6196):566–570, 2014.
- [14] R. A. Satnoianu, M. Menzinger, and P. K. Maini. Turing instabilities in general systems. *J. Math. Biol.*, 41(6):493–512, 2000.
- [15] A. M. Turing. The chemical basis of morphogenesis. *Philos. Trans. Roy. Soc. London Ser. B*, 237(641):37–72, 1952.
- [16] P. van den Driessche. Sign pattern matrices. In *Combinatorial matrix theory*, Adv. Courses Math. CRM Barcelona, pages 47–82. Birkhäuser/Springer, Cham, 2018.

# Modeling Population Dynamics in Stream Environments: Impact of Movement Networks/Matrices

Zhisheng Shuai

Department of Mathematics, University of Central Florida

Orlando, Florida 32816, USA

Yixiang Wu

Department of Mathematics, Middle Tennessee State University

Murfreesboro, Tennessee 37132, USA

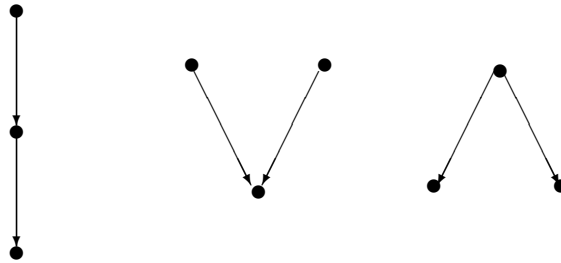
*A Group Project for the CBMS Conference, Orlando, FL, May 2022*

## Objective.

Investigate qualitatively (population persistence/disease invasion) and quantitatively (population biomass/disease endemicity) the impact of movement networks/matrices on spatially heterogeneous populations in stream environments.

## **Problem O** (*Everything starts with zero*)

Assume the network of  $n$  nodes (patches) corresponding to a given stream environment has no cycles of length greater than 2. We thus call this as a *stream network*. There are 3 configurations for stream networks of 3 nodes (as depicted in the following; this is resulted due to the asymmetric movements: downstream movements are generally larger than upstream movements).



- Q1.** Identify all configurations for stream networks of 4 nodes, 5, 6, etc.
- Q2.** Is there a general formula for the number of these configurations?
- Q3.** Which configuration is more suitable for modeling a river or stream in your hometown?

Spatially heterogeneous populations in a stream environment can be modeled as a coupled system of patch models (sub-systems) on a stream network. It is of both mathematical and biological interests to investigate the impact of movements on the *network population growth rate* (i.e.,  $r = s(J)$ , the spectral bound of a certain Jacobian matrix, which determines whether populations persist) and when  $r > 0$ , the *total population biomass*  $B$  (is there a natural way to define  $B$ ?). Specifically, the following questions might serve as a starting point.

- Q1.** Which configuration yields to the largest (smallest) value of  $r$ ?
- Q2.** Which configuration yields to the largest (smallest) biomass, given  $r > 0$ ?
- Q3.** When do Q1 and Q2 have the same answer? When do not? Why?

**Problem S** (*Single Species*)

Consider a single species in a stream environment and its population dynamics can be modeled as the following coupled system on a stream network (i.e., a weighted digraph of no cycles of length  $> 2$ )  $(\mathcal{G}, A)$  with movement (weight) matrix  $A = [a_{ij}]_{n \times n}$ :

$$x'_i = r_i x_i \left(1 - \frac{x_i}{K_i}\right) + \alpha \sum_{j=1}^n (a_{ij} x_j - a_{ji} x_i), \quad i = 1, 2, \dots, n. \quad (S)$$

**S1.** Assume that all intrinsic growth rates  $r_i$  are the same (assumption A1) and that all carrying capacity parameters  $K_i$  are the same (assumption A2). Would  $r$  be a constant, regardless of stream networks? How about  $B$ ?

**S2.** Now only assume A1 but different values of  $K_i$  are allowed. Try answering questions Q1, Q2 and Q3, possibly starting with stream networks of 3 nodes ( $n = 3$ ).

**S3.** Now only assume A2 and different values of  $r_i$  exist. Answer questions Q1, Q2 and Q3.

**S4.** Without any assumptions (neither A1 nor A2), what conclusions can your group draw?

**Problem C** (*Competitive Species*)

For this problem, each patch model can be described by either a classic competition system

$$\begin{aligned} u' &= ru(1 - u - \epsilon v), \\ v' &= \gamma v(1 - \epsilon u - v), \end{aligned} \quad (CC)$$

or a different representation (e.g., see [7, 8])

$$\begin{aligned} x' &= rx \left(1 - \frac{x+y}{K}\right), \\ y' &= \gamma y \left(1 - \frac{x+y}{K}\right). \end{aligned} \quad (CD)$$

**C1.** Answer questions Q1, Q2 and Q3 for representation (CC).

**C2.** Answer these questions again for representation (CD).

**C3.** Do answers in C1 and C2 depend on the representation? Why?

**Problem W** (*Waterborne Disease*)

Cholera is a waterborne disease caused by *Vibrio cholerae* that can live and move within a river or stream. A typical cholera model takes the following form

$$\begin{aligned} S' &= \Lambda - \lambda SW - \mu S, \\ I' &= \lambda SW - \gamma I - \eta I - \mu I, \\ R' &= \gamma I - \mu I, \\ W' &= \xi I - \delta W. \end{aligned} \quad (W)$$

**W1.** Assume only pathogen ( $W$ ) move. Answer Q1, Q2 and Q3 in the understanding of the network basic reproduction number and the disease endemicity respectively.

**W2.** There is an analog of reaction-diffusion equation models (continuous structure) to metapopulation (patch) models (discrete structure). Formulate the corresponding PDE model (see, e.g., [5]) and answer questions in W1.

**W3.** What are possible challenges if both pathogen and human movements are allowed in the model? How to address these challenges?

**Remark.** There are two ebooks [2, 3] on modeling population dynamics which you and your group might find helpful. River structures are discussed in [10, 13], stream fish in [6, 9], and possible *seasonal impact* [4, 12, 14]. You might also want to check a survey [11] for the effect of dispersal patterns on stream populations (continuous structure) and recent results [1] for discrete structure (heavily relying on linear algebra!).

## References

- [1] S. Chen, J. Shi, Z. Shuai, and Y. Wu. Two novel proofs of spectral monotonicity of perturbed essentially nonnegative matrices with applications in population dynamics. *SIAM J. Appl. Math.*, 82(2):654–676, 2022.
- [2] R. J. De Boer. *Modeling Population Dynamics: A Graphical Approach*. 2006. <https://tbb.bio.uu.nl/rdb/books/mpd.pdf>
- [3] A. M. de Roos. *Modeling Population Dynamics*. 2019. [https://staff.fnwi.uva.nl/a.m.deroos/downloads/pdf\\_readers/syllabus.pdf](https://staff.fnwi.uva.nl/a.m.deroos/downloads/pdf_readers/syllabus.pdf)
- [4] D. L. DeAngelis, J. C. Trexler, C. Cosner, A. Obaza, and F. Jopp. Fish population dynamics in a seasonally varying wetland. *Ecological Modelling*, 221(8):1131–1137, 2010.
- [5] W. E. Fitzgibbon, J. J. Morgan, G. F. Webb, and Y. Wu. Modelling the aqueous transport of an infectious pathogen in regional communities: application to the cholera outbreak in Haiti. *J. Royal Society Interface*, 17(169):20200429, 2020.
- [6] B. M. Frank, J. J. Piccolo, and P. V. Baret. A review of ecological models for brown trout: towards a new demogenetic model. *Ecology of Freshwater Fish*, 20(2):167–198, 2011.
- [7] H. Jiang, K.-Y. Lam, and Y. Lou. Are two-patch models sufficient? The evolution of dispersal and topology of river network modules. *Bull. Math. Biol.*, 82(10):Paper No. 131, 42, 2020.
- [8] H. Jiang, K.-Y. Lam, and Y. Lou. Three-patch models for the evolution of dispersal in advective environments: Varying drift and network topology. *Bull. Math. Biol.*, 83(10):1–46, 2021.
- [9] C. Laplanche, A. Elger, F. Santoul, G. P. Thiede, and P. Budy. Modeling the fish community population dynamics and forecasting the eradication success of an exotic fish from an alpine stream. *Biological Conservation*, 223:34–46, 2018.
- [10] W. H. Lowe. Landscape-scale spatial population dynamics in human-impacted stream systems. *Environmental Management*, 30(2):225–233, 2002.
- [11] F. Lutscher, E. Pachepsky, and M. A. Lewis. The effect of dispersal patterns on stream populations. *SIAM Review*, 47(4):749–772, 2005.
- [12] B. Rashleigh, M. C. Barber, M. J. Cyterski, J. M. Johnston, R. Parmar, and Y. Mohamoud. Population models for stream fish response to habitat and hydrologic alteration: the cvi watershed tool. *Environmental Protection Agency, office of Research & Development, Athens, GA, USA*, 2004. [https://19january2017snapshot.epa.gov/sites/production/files/2016-02/documents/rashleigh\\_600\\_r04\\_190\\_population\\_models.pdf](https://19january2017snapshot.epa.gov/sites/production/files/2016-02/documents/rashleigh_600_r04_190_population_models.pdf)
- [13] L. Roques and O. Bonnefon. Modelling population dynamics in realistic landscapes with linear elements: A mechanistic-statistical reaction-diffusion approach. *PloS One*, 11(3):e0151217, 2016.
- [14] J. Shaman, M. Spiegelman, M. Cane, and M. Stieglitz. A hydrologically driven model of swamp water mosquito population dynamics. *Ecological Modelling*, 194(4):395–404, 2006.

# Modeling COVID-19 with Testing Regimes

Pauline van den Driessche

Department of Mathematics and Statistics, University of Victoria, Victoria, BC V8W 2Y2, Canada

In the past couple of years, researchers have formulated many mathematical models of COVID-19. To describe the dynamics, of this virus, different types of models have been used: for example, ordinary differential equation models, network models, stochastic models, agent based models. Each type has its assumptions and each relies on data for practical applications, although some are more data intensive than others. Ordinary differential equation models usually take the classical SIR disease model and include other compartments to make the model more realistic for COVID-19. For example, testing rate and isolation rate are included in a model by Gharouni et al. (2022), various vaccination regimes are considered in Saad-Roy et al. (2021), testing and tracing are included in a model by Sturniolo et al. (2021), various public health interventions are modeled by Wu et al. (2020), and Levine and Earn (2022) investigate the effect of face masks. Many more examples can be found on the web. One advantage of ordinary differential equation models is that mathematical theory, especially linear algebra, can often be used to prove some qualitative theoretical results about the model. These usually need to be supplemented with numerical simulations.

Formulate an ordinary differential equation model for COVID-19 that includes testing of all individuals, including those who are susceptible, pre-symptomatic and symptomatic. The two latter classes test positive with different rates, and individuals testing positive are isolated. One suggestion is to modify the formulation in Gharouni et al. (2022), but you could investigate different formulations as your assumptions vary. This blanket testing has been in force at Princeton University, with everyone required to be tested at least weekly until recently when this was changed to monthly.

Analyse your model(s) using tools from linear algebra. For example, find the control reproduction number, consider the sensitivity (or elasticity) of this number to changes in a parameter, and compute target reproduction numbers (see Lewis et al. (2019)) for various means of control. What conclusions can you draw from your model(s)?

## References.

- A. Gharouni et al. Testing and isolation efficacy: insights from a simple epidemic model, 2022. *Bull. Math. Biol.*, 84:66. <https://doi.org/10.48550/arXiv.2107.08259>
- Z. Levine, D.J.D. Earn. Face masking and COVID-19: potential effects of variation on transmission dynamics, 2022. *J. R. Soc. Interface*, 19: 20210781. <https://doi.org/10.1098/rsif.2021.0781>
- M.A. Lewis et al. A general theory for target reproduction numbers with applications to ecology and epidemiology, 2019. *J. Math. Biol.*, 78, 2317–2339. <https://doi.org/10.1007/s00285-019-01345-4>
- C.M. Saad-Roy et al. Epidemiological and evolutionary considerations of SARS-CoV-2 vaccine dosing regimes, 2021. *Science*, 372 (6540): 363-370. <https://doi.org/10.1126/science.abg8663>
- S. Sturniolo et al. Testing, tracing and isolation in compartmental models, 2021. *PLoS Comput. Biol.*, 17(3): e1008633. <https://doi.org/10.1371/journal.pcbi.1008633>
- J. Wu et al. Quantifying the role of social distancing, personal protection and case detection in mitigating COVID-19 outbreak in Ontario, Canada., 2020. *J. Math. Ind.*, 10 (1):15. <https://doi.org/10.1186/s13362-020-00083-3>